

Nucleation and Growth of the Quasi-Ordered Vortex Phase in $\text{Bi}_2\text{Sr}_2\text{CaCu}_2\text{O}_{8+\delta}$

D. Giller^a, A. Shaulov^a, L. Dorosinski^{a,b}, T. Tamegai^c, and Y. Yeshurun^a

^aInstitute of Superconductivity, Bar-Ilan University, Ramat-Gan, Israel

^bNational Metrology Institute, P.K.21, 41470 Gebze-Kocaeli, Turkey

^cDepartment of Applied Physics, The University of Tokyo, Hongo, Tokyo 113-8656, Japan

The time evolution of the vortex structure in a $\text{Bi}_2\text{Sr}_2\text{CaCu}_2\text{O}_{8+\delta}$ crystal is magneto-optically recorded after a sudden change of the external magnetic field applied to the sample. The magneto-optical images reveal dynamic coexistence of a quasi-ordered vortex phase and a transient disordered vortex phase. The front of the quasi-ordered state moves with time toward the sample edges (center) when the field is suddenly increased (decreased), until a quasi-ordered state is established throughout the entire sample, as dictated by thermodynamics. Effects of magnetic relaxation on the growth rate of the quasi-ordered state are discussed.

1. INTRODUCTION

The thermodynamic phase diagram of the vortex matter in high-temperature superconductors is a topic of extensive theoretical and experimental studies [1-15]. Most efforts have been concentrated on the highly anisotropic $\text{Bi}_2\text{Sr}_2\text{CaCu}_2\text{O}_8$ (BSCCO) crystals [5-10,14], revealing the existence of at least three vortex phases: A liquid phase at high temperatures and two distinct solid phases at low temperatures. The two vortex solid phases have been identified as a quasi-ordered lattice below a transition field $B_{ss}(T)$, and a highly disordered solid above it [2-6,10].

So far, most experimental and theoretical efforts have concentrated on the thermodynamic phases and the transitions between them. We have recently called attention to the process of *formation* of the thermodynamic phases, i.e. to the transient vortex states preceding the establishment of the equilibrium, thermodynamic states. Such transient states can be observed, for example, immediately after a sudden exposure of the sample to an external magnetic field [16]. Experiments described in this paper reveal the process of formation of the quasi-ordered

state in BSCCO in two different types of experiment. In the first one, referred to as 'field-step-up', the sample is suddenly exposed to a steady magnetic field smaller than B_{ss} . In the second type of experiment, referred to as 'field-step-down', the sample is initially exposed to an external field larger than B_{ss} , for a long enough time to allow for the establishment of equilibrium disordered state. Then, the field is suddenly reduced to below B_{ss} . The two types of experiment reveal growth of the quasi-ordered state proceeding in opposite directions: From the sample center toward its edge in the first experiment, and from the sample edge toward the center in the second experiment. The description of these growth processes is the topic of this paper.

2. EXPERIMENTAL

The study was carried out on a $1.5 \times 0.7 \times 0.03 \text{ mm}^3$ $\text{Bi}_2\text{Sr}_2\text{CaCu}_2\text{O}_8$ single crystal [17]. The anomalous second peak associated with the transition field, B_{ss} , is around 500 G. Magnetic induction was detected on the sample's surface employing magneto-optically active Iron-Garnet films with in-plane anisotropy [18,19].

Polarized light passing through the indicator changed its polarization as a function of the *local* magnetic induction. About 100 two-dimensional images were captured by a CCD video camera at time intervals of 40 ms.

3. RESULTS AND DISCUSSION

3.1 Field-Step-Up (FSU) experiments

Figure 1 shows the time evolution of the magnetic induction profiles at $T = 20$ K, after a step increase of the external magnetic field, from zero to $B_a = 420$ G. The sharp induction step at the edges is due to surface currents [20]. The profiles shown in Fig. 1 exhibit a sharp change in the slope at points x_f indicated by arrows, (x_f is measured from the sample's center). The point x_f also marks a clear change in magnetic relaxation characteristics, as shown in [16]. The break point x_f moves progressively with time toward the sample's edge. The time dependence of x_f for $B_a = 420, 450,$ and 500 G, is summarized in the inset to Fig. 1. Measurements performed on another sample [16] shows that in the long time limit, after the break point disappears, the induction profiles gradually evolve into a dome-shaped profile characteristic of geometrical barriers and surface currents [21]. This implies the establishment of a quasi-ordered stable state with vanishing bulk currents.

The break in the profile and the change in the relaxation characteristics at x_f indicate a dynamic coexistence of two distinct vortex phases on both sides of x_f . In order to identify the nature of these phases we assert that initially, a disordered vortex state is formed throughout the sample. The origin of this disordered state is the sudden application of the field, forcing the injection of large amount of vortices through the sample edges. As recently pointed out by Paltiel *et al.* [22] surface barriers and/or defects impede 'smooth' entrance of flux lines into the sample, thus creating a *transient* disordered state. Even in the absence of surface imperfections and barriers, it is plausible that the initial

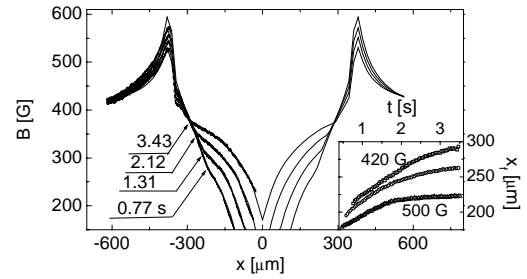


Figure 1. Time evolution of the magnetic induction profiles at $T = 20$ K, after a step increase of the external magnetic field, from zero to 420 G. Arrows denote the location x_f of the breaks in the profiles at the indicated times. Solid lines are fits obtained using the Biot-Savart law. Inset: Time dependence of the break point x_f for $B_a = 420, 450,$ and 500 G.

state of the suddenly injected vortices is a disordered state, as in the presence of bulk defects the vortices cannot arrange themselves immediately in the quasi-ordered state dictated by thermodynamics. As the quasi-ordered state is favored by the thermodynamic conditions, an ordered state starts to nucleate at the sample center, where the field is minimum, and propagates toward the sample edges. This propagation is revealed by the motion of the point x_f on the front of the quasi-ordered state. This motion comes to an halt when x_f reaches the sample edge or, when the induction B_f at x_f reaches the transition field B_{ss} [16].

2.2 Field-Step-Down (FSD) experiments

In a typical experiment of this type we apply a field of 800 G (significantly larger than B_{ss}) and wait long enough time for the establishment of a thermodynamic disordered state in the whole sample. This is manifested by the absence of breaks in the profiles. When this stage is reached, the field is reduced abruptly to 440 G (below B_{ss}). As shown in Figure 2, in this experiment, as in the previous one, the measured induction profiles exhibit a break point x_f where a change in the slope occurs. However, in this case, the break point proceeds toward the sample *center*. The

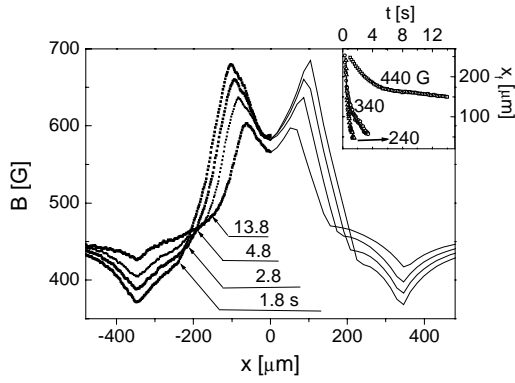


Figure 2. Time evolution of the magnetic induction profiles at $T = 20$ K, after a step decrease of the external magnetic field, from 800 to 440 G. Arrows indicate the breaks in the profiles at the indicated times. Solid lines are fits obtained using the Biot-Savart law. Inset: Time dependence of the break point x_f for $B_a = 440, 340,$ and 240 G.

time dependence of x_f for $B_a = 440, 340,$ and 240 G is summarized in the inset to Fig. 2.

The results of the FSD experiments (Fig. 2) can be interpreted in a similar way as the results of the FSU experiments (Fig. 1). When the field is reduced, the induction profile is partially inverted, causing part of the profile, near the edges, to drop below B_{ss} . The induction is minimum at the edges, thus the ordered phase nucleates at the edges and propagates toward the sample center. At the same time, due to magnetic relaxation, the central part of the profile decreases below B_{ss} , allowing the growth of the quasi-ordered state throughout the entire sample.

The two experiments described above exhibit growth of the quasi-ordered state under different relaxation processes. Nevertheless, in both experiments B_f increases with time. Fig. 3 shows the dependence of B_f on time for different field steps in FSU (open symbols) and FSD experiments. Apparently, in FSU experiments B_f approaches the value of the edge induction, which is determined by external field. In FSD experiments, however, B_f approaches the induction at the center, the value of which continuously decreases with time due to magnetic relaxation. Thus, the

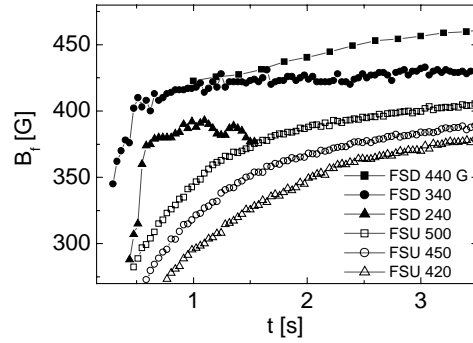


Figure 3. Dependence of B_f on time for different field steps in FSU (open symbols) and FSD experiments.

final value of B_f depends on the time of arrival of x_f to the center. In other words, faster relaxation of the induction at the center implies lower saturation values for B_f .

One of the most important parameters characterizing the growth process is the growth rate $v_f = (dx_f / dt)$, i.e. the velocity of the front of the quasi-ordered state at x_f . Figure 4 shows the time dependence of v_f for different field steps in FSU (open symbols) and FSD experiments. Two features are apparent in Fig. 4. The first is quite expected: The growth velocity decreases with time in all cases. The second observation is the large difference in the growth rate measured in short times in FSU and FSD experiments.

In interpreting the latter observation we note that the above measurements describe the growth process at different stages. It is plausible that we trace the beginning of the growth process in FSD experiments and the tail of this process in FSU experiments. This assumption may be supported by the data in the insets to Figs. 1 and 2, showing that the first measured x_f in FSU experiments is already half way to sample edge. This is because in FSU experiments the velocity of the front is larger at smaller inductions [16,23]; As in FSU experiments the induction at the center always starts from zero, the initial growth is too fast to be detected, and only the tail of the process is traced.

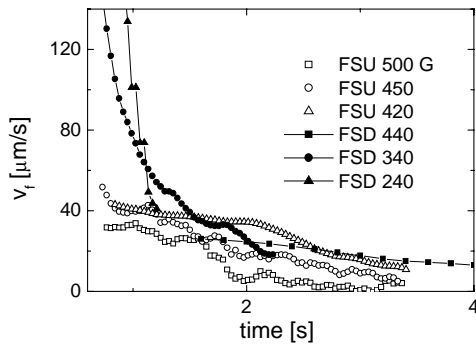


Figure 4. Dependence of v_f on time as measured in different FSU (open symbols) and FSD experiments.

The initial values of v_f have also contribution from the different relaxation conditions in FSU and FSD experiments. In FSU experiments, vortices enter continuously into the sample, causing the induction throughout the entire sample to increase. Thus, B_f can increase even if $v_f = 0$. In contrast, in the FSD experiments vortices continuously exit, causing the induction throughout the entire sample to decrease. Thus, B_f cannot increase unless x_f is moving rapidly toward the center.

4. ACKNOWLEDGEMENTS

This research was supported by The Israel Science Foundation founded by the Israel Academy of Sciences and Humanities - Center of Excellence Program, and by the Heinrich Hertz Minerva Center for High Temperature Superconductivity. Y.Y. acknowledges support from the U.S.-Israel Binational Science Foundation. D. G. acknowledges support from the Clore Foundation. T. T. acknowledges support from a Grant-in-Aid for Scientific Research from the Ministry of Education, Science, Sports and Culture, and from CREST.

REFERENCES

1. G. Blatter, M. V. Feigelman, V. B. Geshkenbein, A. I. Larkin, V. M. Vinokur, *Rev. Mod. Phys.* **66**, 1125 (1994).
2. D. Ertas and D. R. Nelson, *Physica C* **272**, 79 (1996).
3. T. Giamarchi and P. Le Doussal, *Phys. Rev. B* **55**, 6577 (1997).
4. V. M. Vinokur *et al.*, *Physica C* **295**, 209 (1998).
5. R. Cubitt *et al.*, *Nature* **365**, 407 (1993).
6. S. L. Lee *et al.*, *Phys. Rev. Lett.* **71**, 3862 (1993).
7. T. Tamegai, Y. Iye, I. Oguro, and K. Kishio, *Physica C* **213**, 33 (1993).
8. Y. Yeshurun, N. Bontemps, L. Burlachkov, and A. Kapitulnik, *Physical Review B*. **49**, R1548 (1994).
9. A. Schilling *et al.*, *Nature* **382**, 791 (1996).
10. B. Khaykovich *et al.*, *Phys. Rev. Lett.* **76**, 2555 (1996).
11. Y. Yeshurun, A. P. Malozemoff, and A. Shaulov, *Rev. Mod. Phys.* **68**, 911 (1996).
12. K. Kitazawa *et al.*, *Physica C* **282**, 335 (1997).
13. D. Giller *et al.*, *Phys. Rev. Lett.* **79**, 2542 (1997).
14. D. T. Fuchs *et al.*, *Phys. Rev. Lett.* **80**, 4971 (1998).
15. D. Giller, A. Shaulov, Y. Yeshurun, and J. Giapintzakis, *Phys. Rev. B* **60**, 106 (1999).
16. D. Giller, A. Shaulov, T. Tamegai, and Y. Yeshurun, unpublished.
17. N. Motohira *et al.*, *J. Ceram. Soc. Jpn.* **97**, 994 (1989).
18. V. K. Vlasko-Vlasov *et al.*, *Fizika Nizkikh Temperatur* **17**, 1410 (1991).
19. V. K. Vlasko-Vlasov *et al.*, Proceedings of the NATO school "Physics and materials science" on vortex states, flux pinning and dynamics, Eds. R. Kossowsky and S. Bose (1998).
20. M. V. Indenbom *et al.*, *Physica C* **222**, 203 (1994).
21. E. Zeldov *et al.*, *Phys. Rev. Lett.* **73**, 1428 (1994).
22. Y. Paltiel *et al.*, to be published in *Nature* (1999).
23. D. Giller, A. Shaulov, and Y. Yeshurun, Proceedings of the LT22 conference, Helsinki (1999).